

Replication

# [Re] The Evolution of Virulence in Pathogens with Vertical and Horizontal Transmission

Fares Dhane<sup>1,2, ID</sup>, Sandrine Soeharjono<sup>1,2, ID</sup>, Kiri Stern<sup>1,2, ID</sup>, Andrew MacDonald<sup>1, ID</sup>, and Timothée Poisot<sup>1, ID</sup><sup>1</sup>Department of Biology, Université de Montréal, 90 Vincent-d'Indy, Montréal (QC), H2V 2S9, Canada – <sup>2</sup>Equal contributions**Edited by**Nicolas P. Rougier <sup>ID</sup>**Reviewed by**Affan Shoukat  
Stephan Grein <sup>ID</sup>**Received**

09 May 2021

**Published**

22 November 2021

**DOI**

10.5281/zenodo.5722853

**Abstract** The population dynamics of vertical and horizontal transmission allow for the study of the evolution of virulence. Here, we replicate an epidemiological model by Lipsitch et al. (1996) analyzing the trade-offs between both types. The population dynamics between one host and 100 pathogen strains added individually every 1,000 timesteps in the presence of both mechanisms support that increased vertical transmission rates select for lower evolutionary stable levels of virulence. However, virulent vertically-transmitted pathogens can persist when they provide protection against even more virulent horizontally-transmitted strains. Furthermore, increasing horizontal transmission opportunities favour less virulent strains that are good at vertical transmission because of selection for greater host fitness. Finally, we present simulations allowing both transmission rates to evolve, and show that strains exhibiting high levels of vertical transmission can only be successful in contexts of low virulence.

## 1 Introduction

An essential part of parasitic transmission and the evolution of host-pathogen interactions is the mode of transmission. Vertical transmission is the direct transfer of a parasite from one generation to the next during reproduction. Horizontal transmission is the transmission of parasites among related and non-related individuals alike, and can be passed on at any time in the hosts' life cycle<sup>1</sup>. Horizontal transmission can occur directly, such as through air-borne, food-borne or sexual infections, or indirectly through a vector<sup>2</sup>. It has been suggested that these different modes of transmission play a crucial role in determining the virulence of a pathogen<sup>3,4</sup>, which reflects its ability to cause disease<sup>5</sup>. The transmission process thus determines the spread and persistence of a given pathogen in a population, which is crucial to modeling population dynamics and designing proper disease control strategies.

In 1987, Ewald<sup>6</sup> theorized that parasites with predominantly horizontal transmission would tend towards higher virulence, whereas those with vertical transmission would tend towards lower virulence. However, Lipsitch et al. (1996)<sup>7</sup> observed that increased horizontal transmission actually selects for lower virulence and greater vertical transmission in pathogens instead. This occurs because of epidemiological feedback: higher contact rates between hosts allow for a greater number of equilibrium states to be attained, where high horizontal transmission is not effective<sup>8</sup>. This enables strains with lower basic reproductive ratios and vertical transmission to exclude, through competition, those with higher reproductive ratios and horizontal transmission.

In this study, we successfully replicate the epidemiological model incorporating trade-offs between vertical and horizontal transmission from the original study by Lipsitch et al. (1996)<sup>7</sup> using their methods and parameters. This study is foundational in the field of evolutionary epidemiology, in that it challenged the notion that vertical transmission only was able to lower the evolutionarily stable (ESS) level of virulence, which was the

Copyright © 2021 F. Dhane et al., released under a Creative Commons Attribution 4.0 International license.

Correspondence should be addressed to Andrew MacDonald (andrew.macdonald@umontreal.ca)

The authors have declared that no competing interests exist.

Code is available at [https://github.com/BIO6032/2019\\_replication\\_LipstichEtAl\\_1996](https://github.com/BIO6032/2019_replication_LipstichEtAl_1996).

swh:1.dir:c0bcbeb993bac32949bc8f0b2a218673899790e7.

Open peer review is available at <https://github.com/ReScience/submissions/issues/56>.

– SWH

dominant paradigm at the time. We observe the dynamics between 1 host population and 100 infected strains added individually every  $10^3$  time steps for a total of  $10^5$  iterations. This model gives the host population time to stabilize and adapt to the exposure to various pathogens between each transmission opportunity. Different simulations support the idea that vertical transmission is favoured over horizontal transmission in cases of decreased virulence, thus selecting for strains with low virulence. Furthermore, we find that as the number of opportunities for horizontal transmission increase, selection for strains with lower virulence also increases, given that infection is only allowed for one pathogenic strain at a time. Lastly, we present additional simulations in which each strain's properties may evolve through time, thus imitating further realistic conditions. This study was conducted using version 1.6.0 of the Julia programming language.

## 2 Mathematical Model for the Evolution of Virulence

We start by considering a model composed of one uninfected host population and two populations infected with either of two pathogenic strains. This model is a generalization of Lipsitch et al. (1996)<sup>7</sup> single-strain model and its dynamics are governed by the following equations:

$$\frac{dX}{dt} = (b_x X + e_1 Y_1 + e_2 Y_2) \left(1 - \frac{X + Y_1 + Y_2}{K}\right) - u_x X - cX(\beta_1 Y_1 + \beta_2 Y_2) \quad (1)$$

$$\frac{dY_1}{dt} = b_1 Y_1 \left(1 - \frac{X + Y_1 + Y_2}{K}\right) - u_1 Y_1 + c\beta_1 X Y_1 \quad (2)$$

$$\frac{dY_2}{dt} = b_2 Y_2 \left(1 - \frac{X + Y_1 + Y_2}{K}\right) - u_2 Y_2 + c\beta_2 X Y_2 \quad (3)$$

Let  $X$  be the number of uninfected hosts and  $Y_i$  the number of infected hosts with pathogen strains  $i = 1, 2$ . Uninfected hosts have a maximal *per capita* birth rate  $b_x$  and a mortality rate  $u_x$ , resulting in a lifespan of  $(\frac{1}{u_x})$ . Let  $e_i$  represent the *per capita* birth rate of uninfected hosts by hosts infected with strain  $i$  and  $b_i$  represent the *per capita* birth rate of offspring infected with strain  $i$  per unit time. Infected hosts die at the rate  $u_i \geq u_x$ . Let  $c$  be the rate of contact between hosts (i.e. the opportunities for horizontal transmission) and  $\beta_i$  the rate of horizontal transmission of strain  $i$ . Finally, let  $K$  represent the environment's carrying capacity.

For each strain to invade and persist in the population, the basic reproductive rate of the parasite must be greater than 1 and satisfy the following conditions:

$$R_0 = H_0 + V_0 > 1 \quad (4)$$

$$H_0 = \frac{c\beta_i}{u_i} K \left(1 - \frac{u_x}{b_x}\right) \quad (5)$$

$$V_0 = \frac{b_i u_x}{b_x u_i} \quad (6)$$

Where  $H_0$  represents the number of new horizontally-acquired cases from a single infected host in a population of uninfected hosts before the primary host dies and  $V_0$  represents the number of new vertically-acquired cases by the same host introduced into the uninfected population at equilibrium.

Generalizing this two-pathogen model to  $i$  strains allows for the study of more complex dynamics, such as in this epidemiological model replication.

## 2.1 Justification of Parameters

Most parameters used in this study are identical to those in the original study. The initial number of uninfected and infected hosts with strain 1 are of  $X_0 = 80$  and  $Y_{1.0} = 1$ , respectively. We inferred the former from the figures in the original article, since this value was not explicitly mentioned in the text. For the host population, its birth rate  $b_x$  is held constant at 1.0, while its mortality rate  $u_x$  is held constant at 0.2.

For plotting purposes, we set the carrying capacity  $K = 100$  to simulate whole numbers instead of proportions for panels (a,b) of our figures. Also, the values presented in Figures 1-3 comprise of weighted values for  $R_0$ ,  $V_0$ ,  $u_x$ ,  $\beta_i$  and virulence for noise reduction. We set the value of  $K = 1$  in panels (c,d) to simplify the calculation of  $R_0$ . Finally, we plot the evenness of the total population in panels (i,j) of each figure in order to relate it to the evolutionary dynamics of each simulation.

The values for variables  $c$ ,  $b_i$ ,  $e_i$  and  $u_i$  vary between strains and figures in order to compare their different impacts on the epidemiological evolutionary trajectories. The horizontal transmission rate and virulence of each strain are respectively constrained by the following equations:

$$\beta_i(u_i) = \frac{3(u_i - u_x)}{u_i - u_x + 1} \quad (7)$$

$$Virulence = 1 - \frac{(b_i + e_i)u_x}{b_x u_i} \quad (8)$$

Equation (7) defines the monotonically increasing relationship between disease-induced mortality rates  $u_i - u_x$  and horizontal transmissibility. On the other hand, equation (8) defines virulence (ranging from 0 to 1) as the proportional fitness loss of an infected host, where lower virulence equates lower mean mortality.

## 2.2 Figure 1

We compare the evolutionary trajectories with the variable  $b_i$  held constant at the values of 0.1 and 1.0 for every pathogenic strain (thereby calling it a generalized  $b_y$ ) in their respective column. Since the number of infected offspring from an infected host  $e_i$  directly depends on  $b_i$  through the equation  $e_i = b_x - b_i$ , each strain also possesses an  $e_i$  value of 0.9 and 0.0, in each respective case.

## 2.3 Figure 2

We present the evolutionary trajectories with additional variables  $r_1$ ,  $r_2$  and  $r_3$ . Their values are randomly sampled on a uniform distribution over  $[0,1]$  for each strain in order to add stochasticity to the model. They respectively designate the total virulence of the strain, the fraction of virulence attributable to fecundity loss, and the fraction of offspring of infected hosts which are infected. The resulting constraints on the simulations' parameters are the following:

$$e_i = b_x(1 - r_3)(1 - r_1 r_2) \quad (9)$$

$$b_i = b_x r_3(1 - r_1 r_2) \quad (10)$$

$$\beta_i = r_1 - \frac{\alpha b_i}{b_x} \quad (11)$$

Equation 9 mathematically depicts that the birth rate of uninfected offspring by infected hosts  $e_i$  is equal to the maximal *per capita* birth rate  $b_x$  multiplied by the fraction of uninfected offspring  $(1 - r_3)$  minus the fecundity loss due to virulence  $(1 - r_1 r_2)$ . Equation 10

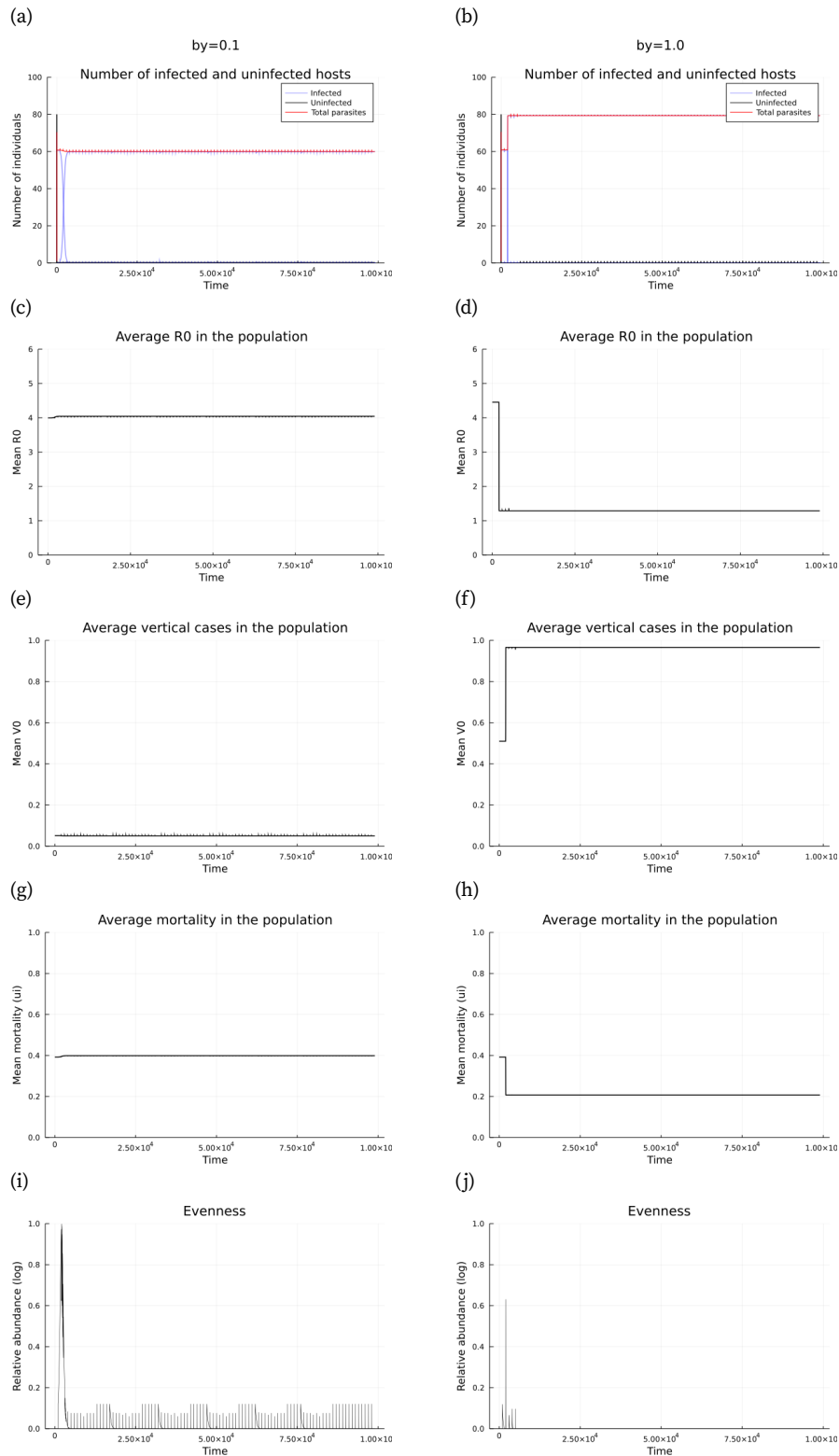


Figure 1. Evolutionary dynamics of 100 infected strains introduced every  $10^3$  generations for two vertical transmission values,  $b_i = 0.1$  (left) and  $b_i = 1.0$  (right). We demonstrate (a,b) the number of uninfected and infected hosts with each strain; (c,d) the mean  $R_0$  in the population; (e,f) the average of all new infections acquired vertically; (g,h) the average mortality in the population; (i,j) the evenness of the total population. We show that higher vertical transmission selects for lower mortality, horizontal transmission and  $R_0$ . Constants:  $c = 4.0$ ,  $b_x = 1.0$ ,  $u_x = 0.2$ ,  $e_i = b_x - b_i$ . Each infected strain possesses a random value of  $u_i \in [u_x, 1]$  which in turn determines its value of  $\beta_i$  according to equation 7. We successfully reproduced Figure 1 from its corresponding figure in the original study. Despite the minor differences due to the random variable permutations, our results follow the same trends.

shows that the birth rate of infected offspring  $b_i$  is equal to the maximal *per capita* birth rate  $b_x$  multiplied the fraction of infected offspring  $r_3$  minus this same loss. Finally, equation 11 reveals that the rate of horizontal transmission  $\beta_i$  is equal to the total virulence  $r_1$  minus the cost of vertical transmission in relation to horizontal transmission  $\alpha$  multiplied by the fraction of infected births  $b_i/b_x$ . We set the parameter  $\alpha$  as a random value over  $[0,1]$  for each strain, introducing a cost-benefit trade-off between vertical and horizontal modes of transmission on parasite fitness. We ensure non-negative horizontal transmission values by setting  $\beta_i$  to zero if the second term happens to be greater than the first term by chance.

## 2.4 Figure 3

We show the evolutionary trajectories where both vertical and horizontal transmission parameters can vary with a constraint. All parameters are identical to those in Figure 2, with the exception of  $r_3$  restricted by the range  $[0, r_1]$  such that the fraction of infected offspring from infected hosts may not exceed the total virulence.

## 3 Discussion

### 3.1 Parameter Constraints

In Figure 1, we replicate the evolutionary trajectories for two different values of vertical transmission,  $b_y = 0.1$  and  $1.0$ , which are held constant for all strains. This scenario represents a case of imperfect vertical transmission such that there is no net loss of fertility due to infection. In other words, virulence (i.e. the loss of fitness of the host) depends solely on mortality through equation (8); we thus neglect the decrease in fitness from the reduction of the number of uninfected offspring.

In the following two figures, we replicate simulations of the evolutionary dynamics with varying vertical and horizontal parameters under constraints through equations (9-11). In Figure 2, strains are permitted to have very low virulence and very high vertical transmission (through random variables  $r_1, r_2, r_3$  and  $\alpha$ ). This state is typically seen in the evolution of avirulence. In Figure 3, high levels of vertical transmission are only permitted with high levels of virulence through the  $r_3 \in [0, r_1]$  restriction. This is typically associated with pathogens that require sufficient replication within the host, usually resulting in the harming of the host.

### 3.2 Analysis of Results

As shown in Figure 1, different parasitic strains persist due to coexistence and competitive exclusion, which varies in degree at every new generation. Similarly to the results observed by Lipsitch et al. (1996)<sup>7</sup>, higher vertical transmission selects for lower mortality, horizontal transmission and  $R_0$ . This indicates a lesser importance of the horizontal transmission parameter, in the case where there is a higher vertical transmission rate; this represents a situation in which the population is saturated with individuals infected by pathogens with high vertical transmission and low virulence. Additionally, lower virulence results in lower mean mortality through equation 8 and as observed in panels (g, h). Panels (i,j) describe the evenness of the total population, which is observed to remain at low values in both situations. Because of the high reproductive rate ( $R_0 > 1$ ), a small number of strains occupy the majority of the population, while close to no hosts remain uninfected.

Figure 2 shows the evolutionary trajectories where high vertical transmission is compatible with low virulence. Two cases with identical parameters except for the rate of contact between hosts,  $c = 0.5$  and  $c = 4.0$ , are presented. As predicted in the original study, an increase in the contact rate selects for less virulent strains exhibiting high vertical

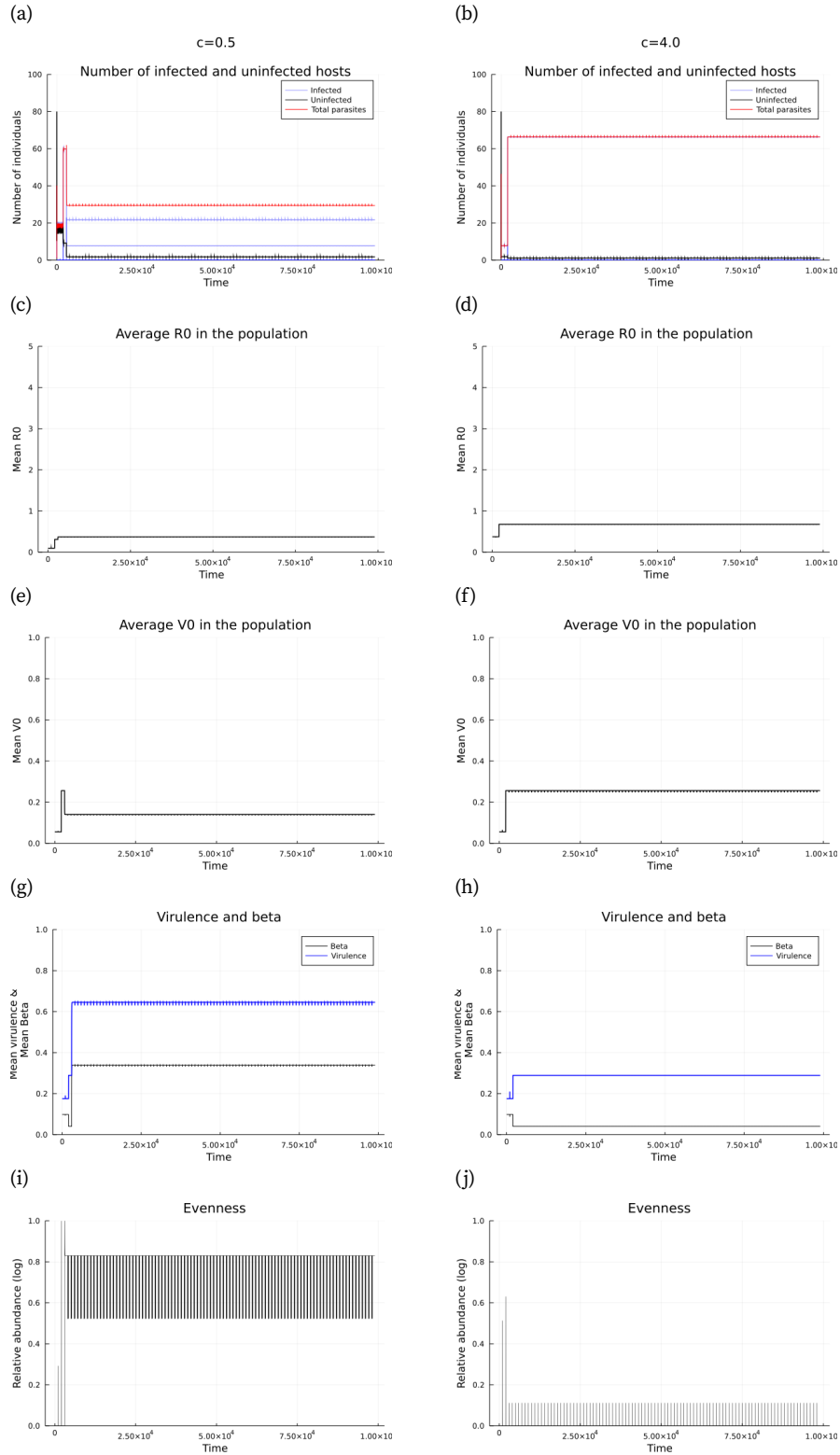
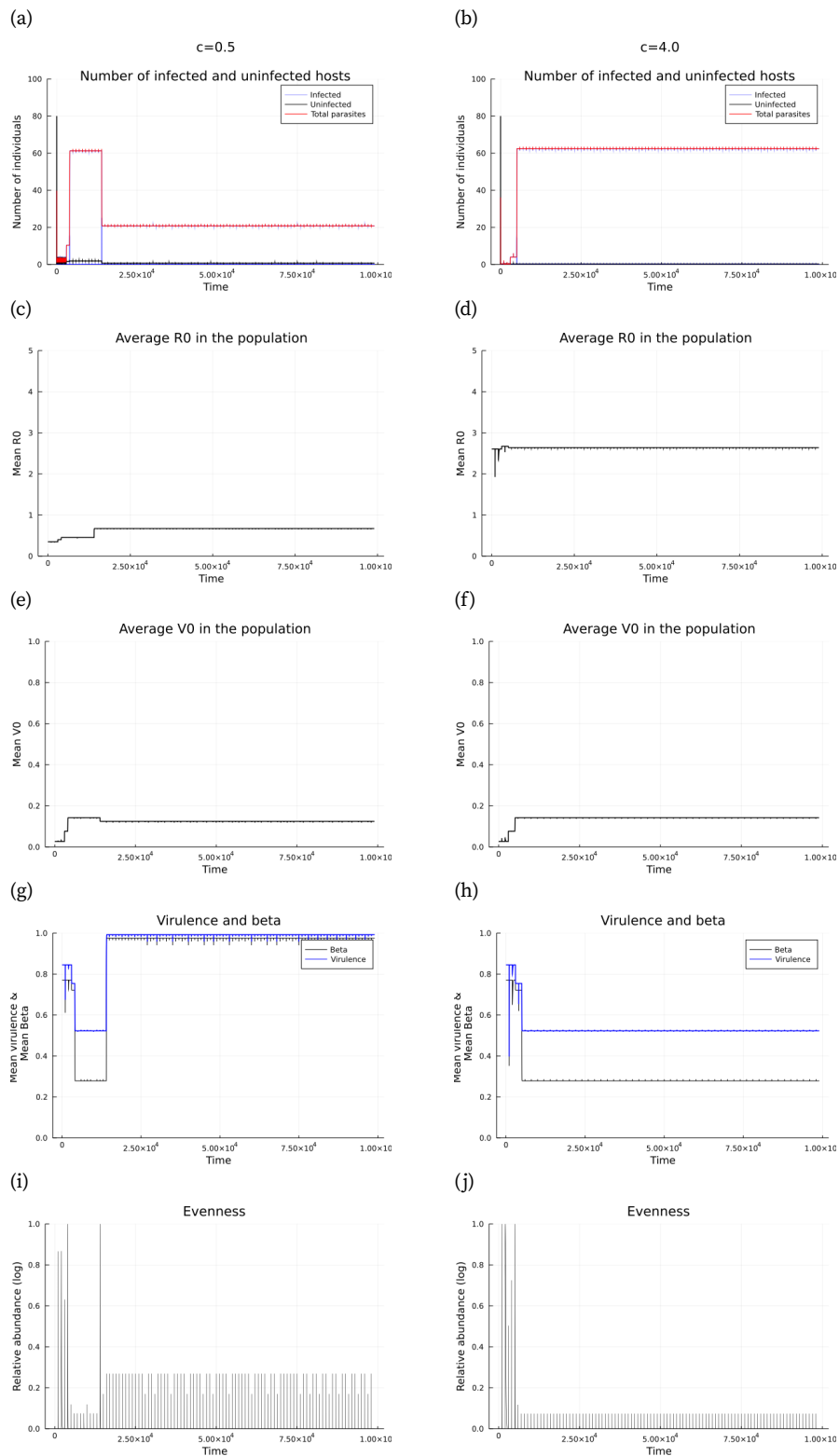


Figure 2. Evolutionary dynamics of 100 infected strains introduced every  $10^3$  generations for two horizontal transmission opportunity,  $c = 0.5$  (left) and  $c = 4.0$  (right). The parameters are identical to those in Figure 1 but with constraints from equations (9), (10) and (11). We demonstrate (a,b) the number of uninfected and infected hosts with each strain; (c,d) the mean  $R_0$ ; (e,f) the average of all new infections acquired vertically; (g,h) the average virulence and horizontal transmission rate  $\beta_i$ ; (i,j) the evenness of the total population. We show that a higher contact rate  $c$  selects for lower virulence at equilibrium and higher vertical transmission rates. The variability induced by the parameters allows for strains of high vertical transmission and low virulence to persist. Constants:  $b_x = 1.0$  and  $u_x = 0.2$ . Each infected strain possesses a random value of  $u_i \in [u_x, 1]$ . We successfully reproduced Figure 2 from its corresponding figure in the original study. Although our results follow the same trends, our simulations demonstrate lower values of  $V_0$ , virulence and  $\beta_i$ , on top of minor differences due to stochasticity.



**Figure 3.** Evolutionary dynamics of 100 infected strains introduced every  $10^3$  generations for two values of horizontal transmission opportunity,  $c = 0.5$  (left) and  $c = 4.0$  (right). All parameters are identical to those in Figure 2 but with a constraint  $r_3$  chosen randomly from a uniform distribution over  $[0, r_1]$  per strain. We demonstrate (a,b) the number of uninfected and infected hosts with each strain; (c,d) the mean  $R_0$ ; (e,f) the average of all new infections acquired vertically; (g,h) the average virulence and horizontal transmissibility  $\beta_i$ ; (i,j) the evenness of the total population. Similarly, we show that a higher contact rate  $c$  selects for lower virulence and higher vertical transmission rates. However, higher levels of virulence evolve and an increase in vertical transmission results in little fitness benefit. We successfully reproduced Figure 3 from its corresponding figure in the original study. Our results follow the same trends, although our simulations for  $c = 4.0$  demonstrate lower values of  $R_0$  and  $V_0$ .

transmission rates. This can be explained by the fact that as the number of contacts between individuals increases, the number of available susceptible individuals decreases, leading to saturation.

Figure 3 describes an equilibrium similar to that of Figure 2, but with increases in virulence. This can be explained through the limit on vertical transmission (through the constraint  $r_3 \in [0, r_1]$ ) and the low rate of horizontal transmission, which is directly correlated to the contact rate ( $c = 0.5$ ). Equation 4 confirms this observation, where the invasion and persistence of a parasite can only occur when the sum of  $H_0$  and  $V_0$  is greater than 1. Selection thus favours parasites exhibiting relatively high virulence and employing horizontal transmission. As previously described, the fraction of infected offspring from infected hosts, and thus vertical transmission, is limited by the total virulence of the strain. This constraint results in the mean  $V_0$  barely attaining a vertical basic reproductive ratio of 0.2, thus demonstrating the limited fitness benefit conferred by vertical transmission. We therefore confirm the results from Lipsitch et al. (1996)<sup>7</sup>, where horizontal transmission is less virulent than vertical transmission. Our simulations show that natural selection will always select for strains of lower virulence, which explains the decrease in virulence shown in panels (g,h).

In Figures 2 and 3, selection for the type of transmission will depend on whether high vertical transmission is limited by virulence. When there is a competition between both transmission types, there will always be selection for the type that guarantees greater host fitness. And as seen in Ebert and Bull (2003), vertically-transmitted strains are less virulent than horizontally-transmitted ones. A horizontally-transmitted strain will always push the host to invest its energy in contact rather than reproduction, while vertical transmission ensures the opposite. A less virulent strain using vertical transmission provides the host with greater fitness than a very virulent strain using horizontal transmission, which therefore guarantees its persistence in the population over time. This dynamic is reflected in the relationship between virulence and the type of transmission<sup>9</sup>. However, in the case where high vertical transmission requires high virulence, horizontally-transmitted pathogens would prevail because of the low fitness benefits from vertical transmission.

### 3.3 Other Remarks

In this replication study, we observe fewer variation and trade-offs between competing strains in panels (a,b) of Figures 1-3, since the infected persist faster and certain dominant strains take over the entire population for the remainder of the simulations. We also notice generally lower  $R_0$  and  $V_0$  values than expected from the simulations in Lipsitch et al. (1996)<sup>7</sup>. This could be attributed to the variability induced by the four random variables  $r_1$ ,  $r_2$ ,  $r_3$  and  $\alpha$  (where the latter in particular was chosen as a random value over  $[0,1]$  per strain due to a lack of information in the original study) or to potentially different initial numbers of individuals (which were also arbitrarily chosen due to their values not being explicitly mentioned in the text). It could also be explained by the differences in duration of the simulations; this replication was done on a smaller scale, with ten times less strains, such that the probability of one random strain overcoming the one with the highest fitness is reduced by a factor of ten. Finally, we note that the population evenness is inversely related to the presence of dominant strains; very few strains monopolizing the population result in low evenness, whereas multiple strains co-existing result in a population exhibiting higher evenness. Panels (i,j) of each figure depict the expected dynamics in such cases.

### 3.4 Conclusion

Few models consider the evolution of virulence for parasites with mixed horizontal and vertical transmission. Here, our results are similar to the findings of Lipsitch et al. (1996)<sup>7</sup>, suggesting that selection depends on whether high vertical transmission rates



are constrained by low or high virulence. Similarly, we observed that selection favours vertically-transmitted strains, but only when vertical transmission is compatible with low virulence. On the other hand, in situations where high vertical transmission rates are only possible with high virulence, horizontal transmission is favoured. Ultimately, selection will always favour the least virulent strain, regardless of the type of transmission.

These findings could suggest that efforts to reduce vertical transmission of pathogens could, unintentionally, shift selection towards mutants of increased virulence. It is possible that vertical transmission has placed a selection pressure on pathogens to evolve at relatively low levels of virulence, thereby allowing the mother-to-offspring chain of transmission to continue over several generations. However, in cases where the horizontal transmission rates are also low, reducing vertical transmission might be sufficient to eliminate a pathogen from a population by bringing its basic reproductive ratio below unity.

## References

1. D. Ebert. "The Epidemiology and Evolution of Symbionts with Mixed-Mode Transmission." In: **Annual Review of Ecology, Evolution, and Systematics** 44.1 (2013), pp. 623–643. doi: 10.1146/annurev-ecolsys-032513-100555. eprint: <https://doi.org/10.1146/annurev-ecolsys-032513-100555>. URL: <https://doi.org/10.1146/annurev-ecolsys-032513-100555>.
2. Y. Chen, J. Evans, and M. Feldlaufer. "Horizontal and vertical transmission of viruses in the honey bee, *Apis mellifera*." In: **Journal of Invertebrate Pathology** 92.3 (2006). Society of Invertebrate Pathology 2006 Special Issue, pp. 152–159. doi: <https://doi.org/10.1016/j.jip.2006.03.010>. URL: <http://www.sciencedirect.com/science/article/pii/S0022201106000814>.
3. D. H. Clayton and D. M. Tompkins. "Ectoparasite virulence is linked to mode of transmission." In: **Proceedings of the Royal Society of London. Series B: Biological Sciences** 256.1347 (1994), pp. 211–217. doi: 10.1098/rspb.1994.0072. eprint: <https://royalsocietypublishing.org/doi/pdf/10.1098/rspb.1994.0072>. URL: <https://royalsocietypublishing.org/doi/abs/10.1098/rspb.1994.0072>.
4. P. W. Ewald. "Genetics and evolution of infectious diseases." In: **The Lancet Infectious Diseases** 11.10 (2011), p. 739. doi: [https://doi.org/10.1016/S1473-3099\(11\)70271-7](https://doi.org/10.1016/S1473-3099(11)70271-7). URL: <http://www.sciencedirect.com/science/article/pii/S1473309911702717>.
5. S. Payne. "Chapter 9 - Viral Pathogenesis." In: **Viruses**. Ed. by S. Payne. Academic Press, 2017, pp. 87–95. doi: <https://doi.org/10.1016/B978-0-12-803109-4.00009-X>. URL: <http://www.sciencedirect.com/science/article/pii/B978012803109400009X>.
6. P. W. EWALD. "Transmission Modes and Evolution of the Parasitism-Mutualism Continuum." In: **Annals of the New York Academy of Sciences** 503.1 (1987), pp. 295–306. doi: <https://doi.org/10.1111/j.1749-6632.1987.tb40616.x>. eprint: <https://nyaspubs.onlinelibrary.wiley.com/doi/pdf/10.1111/j.1749-6632.1987.tb40616.x>. URL: <https://nyaspubs.onlinelibrary.wiley.com/doi/abs/10.1111/j.1749-6632.1987.tb40616.x>.
7. M. Lipsitch, S. Siller, and M. A. Nowak. "THE EVOLUTION OF VIRULENCE IN PATHOGENS WITH VERTICAL AND HORIZONTAL TRANSMISSION." In: **Evolution** 50.5 (1996), pp. 1729–1741. doi: <https://doi.org/10.1111/j.1558-5646.1996.tb03560.x>. eprint: <https://onlinelibrary.wiley.com/doi/pdf/10.1111/j.1558-5646.1996.tb03560.x>. URL: <https://onlinelibrary.wiley.com/doi/abs/10.1111/j.1558-5646.1996.tb03560.x>.
8. M. Lipsitch, M. A. Nowak, D. Ebert, and R. M. May. "The population dynamics of vertically and horizontally transmitted parasites." In: **Proceedings of the Royal Society of London. Series B: Biological Sciences** 260.1359 (1995), pp. 321–327. doi: 10.1098/rspb.1995.0099. eprint: <https://royalsocietypublishing.org/doi/pdf/10.1098/rspb.1995.0099>. URL: <https://royalsocietypublishing.org/doi/abs/10.1098/rspb.1995.0099>.
9. B. R. Levin. "The evolution and maintenance of virulence in microparasites." In: **Centers for Disease Control** 2.2 (1996), pp. 93–102. doi: 10.3201/eid0202.960203. URL: <http://www.sciencedirect.com/science/article/pii/S1473309911702717>.

## 4 Supplementary Figures

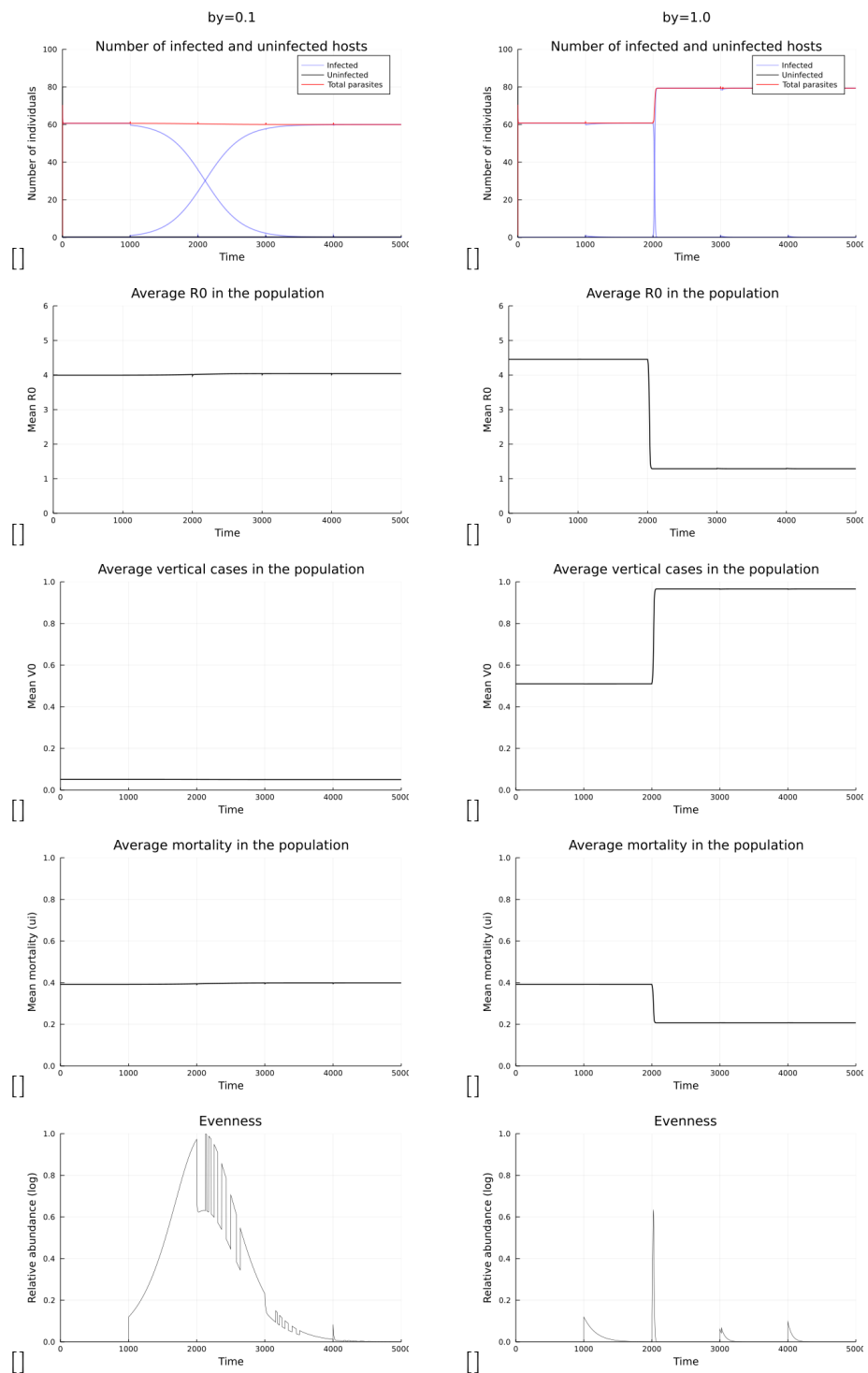


Figure S1. Same evolutionary dynamics as seen in Figure 1 plotted for 5,000 time-steps only.

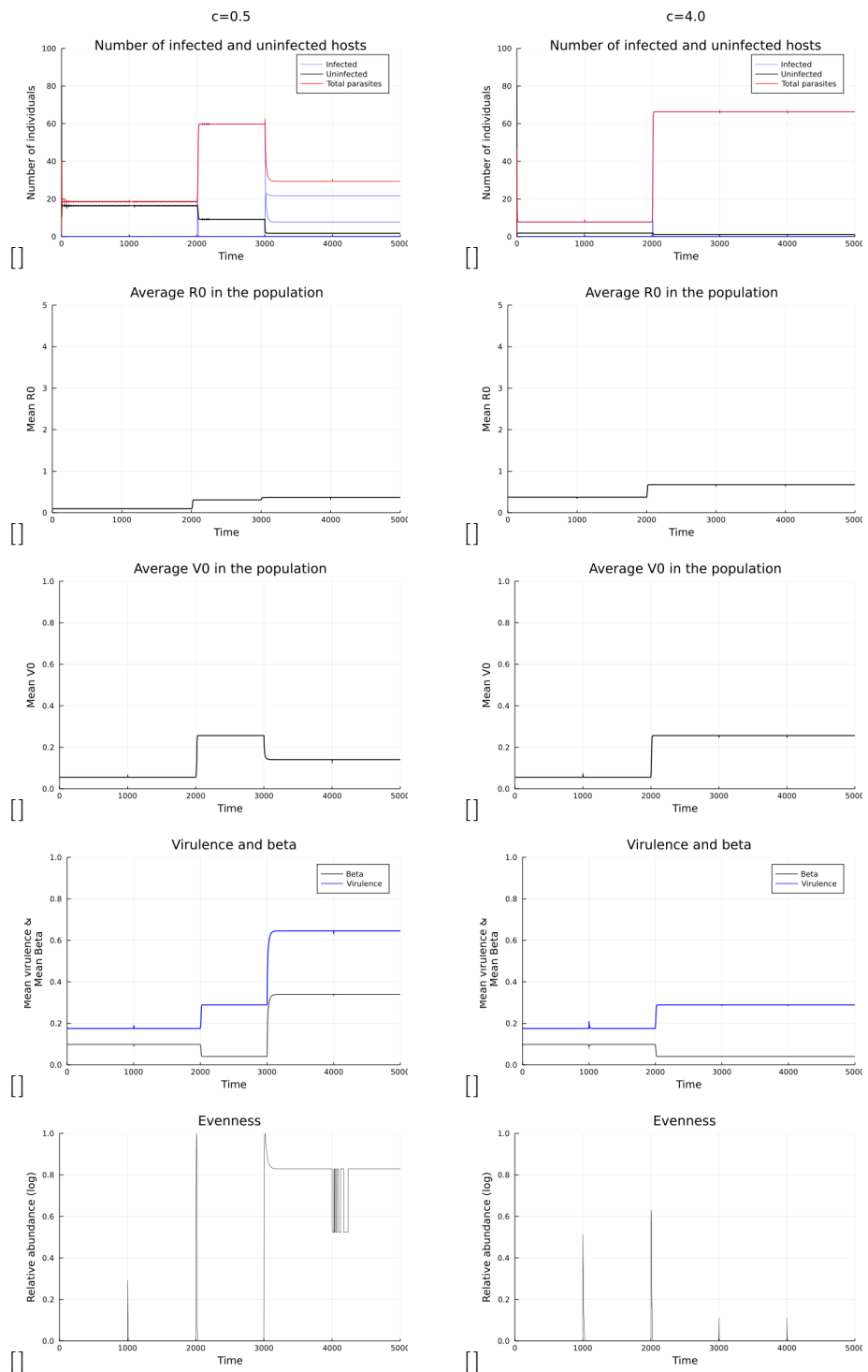


Figure S2. Same evolutionary dynamics as seen in Figure 2 plotted for 5,000 time-steps only.

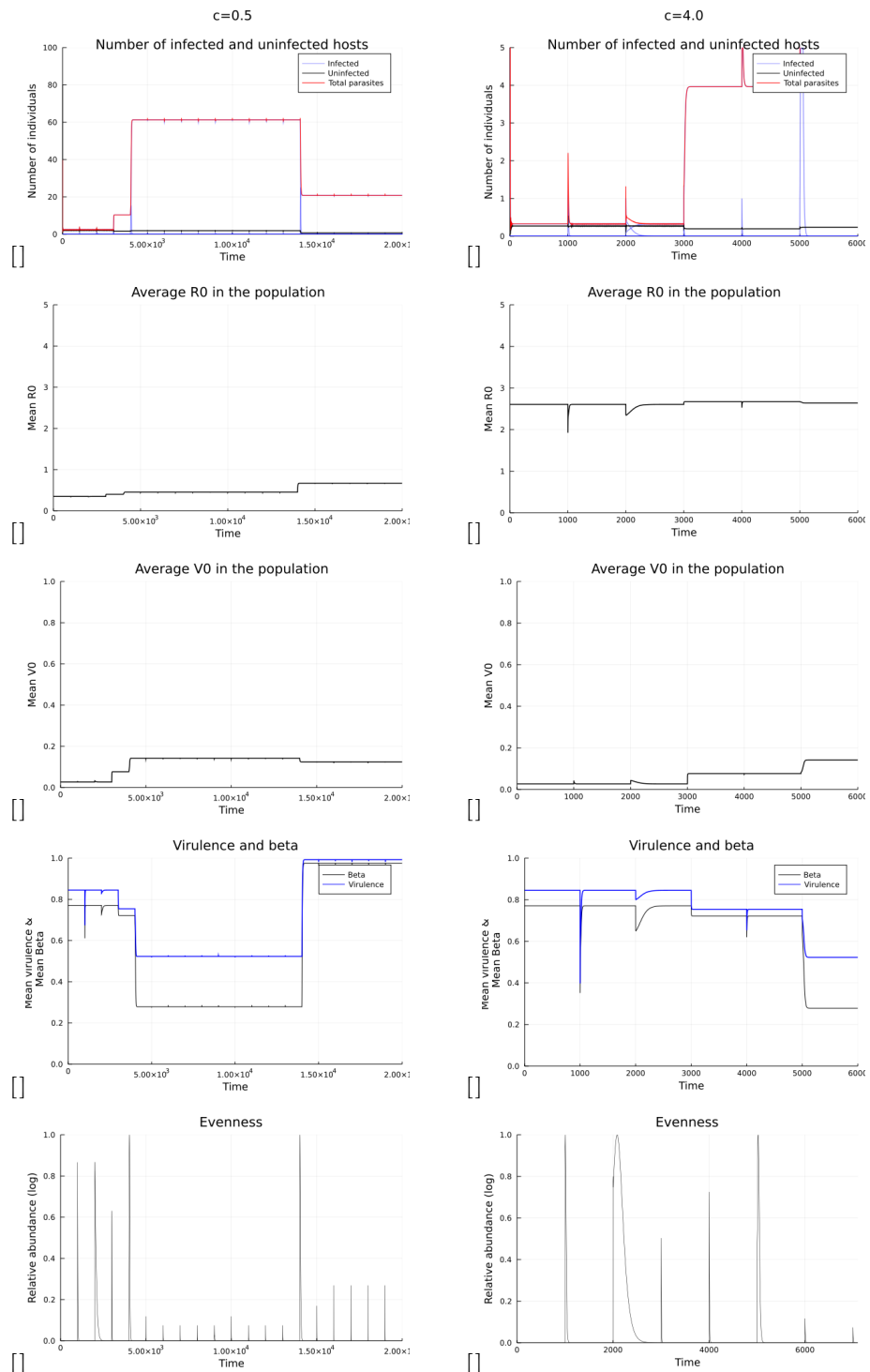


Figure S3. Same evolutionary dynamics as seen in Figure 3 plotted for only 20,000 and 6,000 time-steps for left and right column, respectively.